

International Conference on Space Optics—ICSO 2008

Toulouse, France

14–17 October 2008

Edited by Josiane Costeraste, Errico Armandillo, and Nikos Karafolas



PERSEE: a nulling interferometer with dynamic correction of external perturbations

S. Jacquinod

K. Houairi

J.-M. Le Duigou

M. Barillot

et al.



PERSEE: A NULLING INTERFEROMETER WITH DYNAMIC CORRECTION OF EXTERNAL PERTURBATIONS

S. Jacquinod⁽¹⁾, K. Houairi⁽²⁾⁽³⁾⁽⁸⁾, J.M. Le Duigou⁽³⁾, M. Barillot⁽⁴⁾, F. Cassaing⁽²⁾⁽⁸⁾, J.M. Reess⁽⁵⁾⁽⁸⁾, F. Henault⁽⁶⁾, B. Sorrente⁽²⁾⁽⁸⁾, G. Morinaud⁽¹⁾, J.P. Amans⁽⁷⁾⁽⁸⁾, V. Coudé du Foresto⁽⁵⁾⁽⁸⁾, M. Ollivier⁽¹⁾

⁽¹⁾Institut d'Astrophysique Spatiale, Bt. 121, Université Paris-Sud, 91405 Orsay Cedex, France, sophie.jacquinod@ias.u-psud.fr, marc.ollivier@ias.u-psud.fr

⁽²⁾ONERA DOTA, 29 Av. de la Division Leclerc, BP 72, 92322 Chatillon, France, kamel.houairi@onera.fr

⁽³⁾Centre National d'Etudes Spatiales, 18 Av. E. Belin, 31401 Toulouse, France, jean-michel.leduigou@cnes.fr

⁽⁴⁾Thales Alenia Space, 100 Bd. Du Midi, 06322 Cannes-la-Bocca, France, marc.barillot@thalesaleniaspace.com

⁽⁵⁾LESIA, Observatoire de Paris, 5 place J. Janssen, 92195 Meudon Cedex, France, jean-michel.reess@obspm.fr

⁽⁶⁾Observatoire de la Côte d'Azur, Av. N. Copernic, 06130 Grasse, France, francois.henault@obs-azur.fr

⁽⁷⁾GEPI, Observatoire de Paris, 5 place J. Janssen, 92195 Meudon Cede, France, J.P.Amans@obspm.fr

⁽⁸⁾PHASE, the high angular resolution partnership between ONERA, Obs. De Paris, CNRS & Univ. Denis Diderot Paris

ABSTRACT

Nulling interferometry is one of the direct detection methods assessed to find and characterize extrasolar planets and particularly telluric ones. Several projects such as Darwin [1;2], TPF-I [3;4], PEGASE [5;6] or FKSI [7], are currently considered. One of the main issues is the feasibility of a stable polychromatic null despite the presence of significant disturbances, induced by vibrations, atmospheric turbulence on the ground or satellite drift. Satisfying all these requirements is a great challenge and a key issue of these missions. In the context of the PEGASE mission, it was decided (in 2006), to build a laboratory demonstrator named PERSEE. It is the first laboratory setup which couples deep nulling interferometry with a free flying GNC simulator [8]. It is developed by a consortium composed of CNES, IAS, LESIA, OCA, ONERA, and TAS. In this paper, we detail the main objectives, the set-up and the function of the bench. We describe all the sub-systems and we focus particularly on two key points of PERSEE: the beam combiner and the Fringe tracker.

1. INTRODUCTION

PERSEE (Pegase Experiment for Research and Stabilization of Extreme Extinction) [8] laboratory test bench has been under development since 2006 by a consortium composed of Centre National d'Etudes Spatiales (CNES), Institut d'Astrophysique Spatiale (IAS), Observatoire de Paris-Meudon (LESIA), Observatoire de la Côte d'Azur (OCA), Office National d'Etudes et de recherches Aéronautiques (ONERA), and Thales Alenia Space (TAS) who shared its experience on MAII [9]. It is funded by CNES R&D. The aim of PERSEE is to couple a nulling interferometer with a free flying Guidance Navigation and Control (GNC) simulator. In this paper, we present a general description of PERSEE with a focus on two sub-systems.

2. OVERALL DESCRIPTION OF PERSEE

2.1 Detailed objectives

The idea of PERSEE is to couple a nulling interferometer with a free flying Guidance Navigation and Control (GNC) simulator allowing introducing realistic disturbances and correcting them with active internal loops controlling the optical path difference (opd) and the pointing [8]. Therefore, PERSEE includes a nuller (a beam combiner and a detection), a co-phasing system (a Star Tracker system (ST) and a Fringe Tracker (FT)) and a perturbation injection system. The aim is to achieve all of the detailed objectives listed below:

- Produce an average null of 10^{-4} with a stability of 10^{-5} over a few hours in the spectral range from 1.65 to 3.3 μm
- Validate the fringe acquisition with a drift speed up to 150 $\mu\text{m/s}$
- Determine the external noise acceptable for the two active loops on tip/tilt and opd
- Study the interaction between the opd/tip-tilt/flux loops
- Demonstrate the differential stability between the nuller and the co-phasing sensor
- Develop the calibration procedures, basing on measurements produced by the co-phasing loops
- Validate the global operation with realistic external perturbations in all modes: tracking, star/fringe acquisition, unloading of small-stroke fine correctors
- Study the effects of polarization induced by variations of the angles of incidence on each arm of the interferometer due to external perturbations and affecting the nulling performance.

2.2 Working spectral range

PERSEE being the laboratory test bench designed to study the feasibility of the PEGASE mission, the spectral band was chosen to be as representative as

possible of PEGASE and to take all the constraints into account. PERSEE's spectral range is 0.6 to 3.3 μm . The lower limit of the band is imposed by the gold coating of the mirrors.

The scientific domain covers the range from 1.65 to 3.3 μm . It has been shifted with respect to the scientific range of PEGASE ([2.5 – 5] μm) to reduce cost but similar relative width was maintained (one octave). Had we wanted to go beyond 3.3 μm , we would have had to use a very efficient detector (such as the HAWAI type) and it would have been too expensive. The band is divided in 5 sub-bands. We have 4 channels between 1.65 and 2.5 μm and one between 3.0 and 3.3 μm . They are used to perform nulling measurements. The channel between 2.5 and 3.0 μm is unused due to water absorption. The spectral resolution is $R=10$.

The co-phasing system covers the range from 0.6 to 1.5 μm . The identification of the central fringe is performed in two channels by the FT: [0.8 – 1.0] μm and [1.0 – 1.5] μm . The [0.6 – 0.8] μm band was originally dedicated to the Star Tracker system but the [0.8 – 1.0] μm is now preferred because the source initially planned is not suitable.

Table 1 summarizes the distribution of the spectral sub-bands of PERSEE and their astronomical conventional designations.

Table 1: Spectral bands of PERSEE

Wavelength (μm)	Allocation	Name
[0.6 – 0.8]	Ancient ST channel	R
[0.8 – 1.0]	FT channel 1 + ST channel	I
[1.0 – 1.5]	FT channel 2	J
[1.65 – 2.5]	IR Scientific channels (4)	H + K
[3.0 – 3.3]	IR Scientific channel 5	L

3. OPTICAL SET-UP

PERSEE is composed of several modules presented in the Fig. 2. Their description and function are detailed below. Fig. 1 shows the CAD model of the main optical bench, designed by TAS (July 2008).

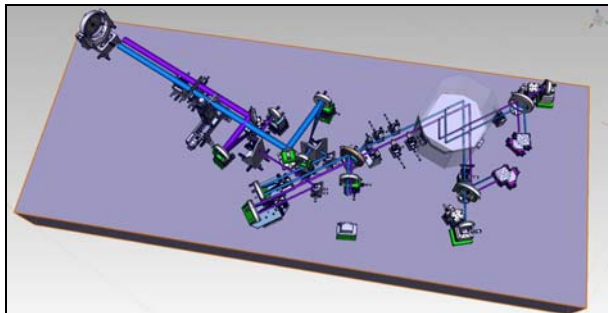


Fig. 1: CAD model of the main optical bench of PERSEE (TAS courtesy)

3.1 Source and separation modules

Relying on the SNR analysis and the trade-off study of PERSEE, it has been shown that it was impossible to

cover the whole spectral range of PERSEE with a single source. Therefore, the source module comprises two subsystems.

The source allowing to simulate the observed central star (H, K and L bands) is a Xenon lamp (5000K). In order to ensure good spatial coherence and high wavefront quality, the light is injected into a single-mode fiber (SMF) in fluorid glass from Le Verre Fluoré with a cut-off wavelength of 1.65 μm .

The co-phasing system (I and J bands) uses a combination of laser diodes. They are injected into silica SMFs. The fibers also allow to place the sources on a dedicated bench, not to disturb the stability of the main optical bench.

The fibers arrive at the focus of a parabolic collimator ($f = 0.75 \text{ m}$). They are firmly linked by a dedicated connector designed to assure a stable spacing between the axes of the fibers. Their separation is along a vertical axis, this ensure that it is unresolved by the horizontal interferometer baseline.

To delimit the two PERSEE's beams, we use the principle of wavefront separation. A mask is placed at the output of the parabola to produce the beams.

3.2 Optical train

After the separation system, the two beams follow identical paths along the optical train (cf. Fig. 2). All mirrors are coated with unprotected gold.

The M1 flat mirrors, turned by 45° , represent the siderostats of a Bracewell type space interferometer such as PEGASE. They are mounted on piezo-systems to inject disturbances on tip/tilt and opd (detailed description in §3.4).

M2 and M3 (parabolic mirrors) form symmetric off-axis afocal systems to perform beam compression. We cannot represent the real magnification of PEGASE ($M = 20$), thus we will use a scale factor to extrapolate results to real systems. The trade-off study led to $M = 3$, because of the limited allowable inertia of M1 (perturbation injection) and of the coupling of injected tip/tilt disturbances at this level with the flux mismatch (gaussian output of the collimator). The diameter beam passes from 40 mm after M1 to 13 mm after M3.

The folding mirrors M4 and M5 orient the beams in the good direction. Another function of this periscope is that the combination of M4 and M1 form a geometrical achromatic π phase shifter (APS) or field reversal APS. As the π -APS, required for the achromatic null, is naturally present in the optical design, PERSEE will first test this solution. Furthermore, a more classical system based on dispersive sliding prisms (such as those tested on SYNAPSE [10] and MAII [9] benches) is implemented before the combination stage to correct any defaults of differential chromatism. In case of unexpected problems (alignment, polarization), it can be converted into a π -APS and the geometrical APS removed.

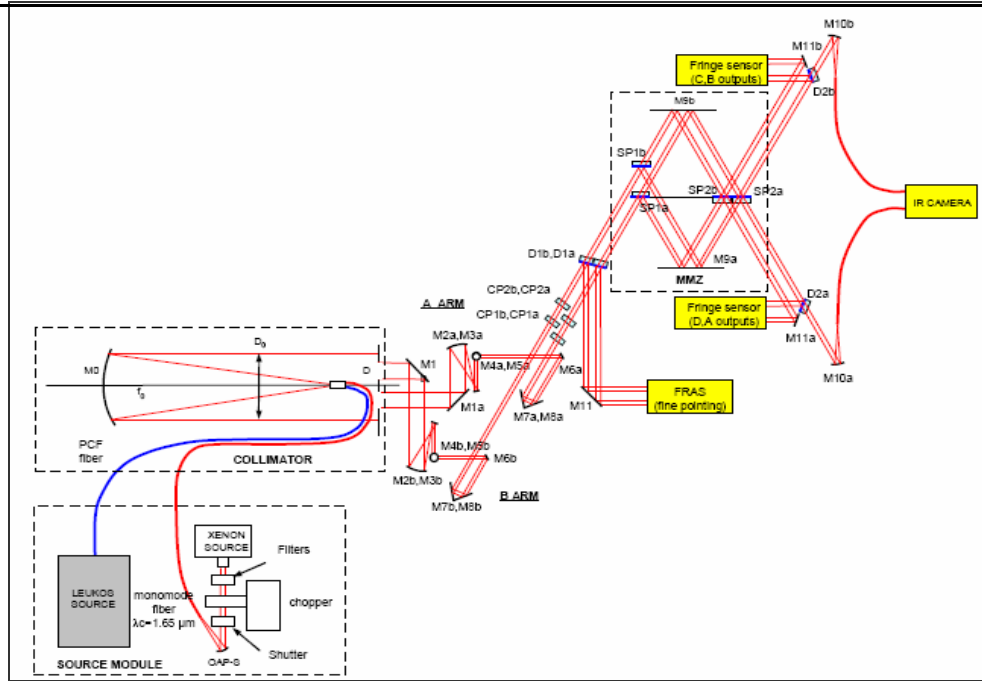


Fig. 2: Optical design of PERSEE (designed by TAS in June 2008)

M6a et b are flat mirrors, turned by 30° to minimize the effects of differential polarization coming from their different positions. The mirrors are mounted on very precise piezo-system to correct perturbations. They are a part of the correction stage detailed in §3.4.

The optical delay lines (ODL) have a cat's eye geometry. They are composed of the parabolic mirrors M7 and the spherical mirrors M8. They are used for opd perturbation or correction, and for pupil imaging.

D1 are annular mirrors. Their goal is to separate the ST band from the others (IR and FT). The outer ring of the beams is reflected toward the ST camera while the main beams go through the inner hole, towards the combination stage. At first, D1 were intended to be dichroic plates to have a transmission on the IR channel (better solution according the optical coating analysis) but the complexity of the coating and the induced chromatism led us to develop another solution.

D2 are dichroic plates. They separate the scientific band from the FT band after the combination. They only influence the nulled output at the SMF injection through the total WFE budget.

M10 Parabolic mirrors inject the destructive and constructive beams into SMFs from Le Verre Fluoré. The beams are sent to the IR camera (cf. §3.7).

The pupil stop is placed just after D1 and reimaged backwards on the M6 mirrors with the cat's eye ODLs.

3.3 Combination stage

This module combines the nuller and the FT system in order to minimize differential paths. The integration of these two functions, which share the same optical components, is a key point of PERSEE [18]. The beam combiner is developed jointly by IAS, CNES and ONERA. It is based on a Modified Mach Zehnder (MMZ) geometry [11]. The incidence angle is 30° .

The concept and the design of the combination stage are detailed in §4.

3.4 Perturbation injection and correction stages

M6 mirrors are mounted on the very precise piezo-system PI S316-10 from Physik Instrumente which allow tip/tilt and translation movement. They are the main correctors for the ST and the FT systems. At first, they will be the only correctors. They will be used to correct for alignment errors (static errors) and laboratory disturbances. Then, they will serve both to introduce and correct small tip/tilt and opd perturbations [12].

Subsequently, M1 mirrors will introduce dynamic perturbations. M1a is mounted on the piezo-system P752 from Newport and will inject small-range opd. M1b is mounted on the piezo-system PI S330 from Physik Instrumente and will introduce tip/tilt.

In a third step, long stroke perturbations of the opd will be introduced using a high resolution (1 nm) and long stroke (1 cm) ODL. First, this will be implemented by the M7-M8 cat's eye mounted on the very precise XMS50 translation stage (Newport). This could be replaced later by a more representative ODL, such as the one developed by TPD-TNO under an ESA R&D contract [13].

Typical profiles of injected perturbations, which drive M1a, M1b and M7-M8a mirrors, are derived from the EADS-ASTRIUM study of the PEGASE GNC (CNES R&d contract [14]).

The measurements used to perform corrections are provided by the Star Tracker camera (cf. §3.5) and the fringe sensor module (cf. §3.6).

3.5 Star Tracker

The ST camera is a IPX-VGA210-L from Imperx.

It is common to both beams. D1 reflect the beams. They go through a common lens (diameter: 50 mm, focal length: 300 mm) towards the camera. The arrangement of the optical components allows reducing the baseline and introducing the differential angle required to separate the images of the two stars on the camera. The useful zone of the camera is a 100x100 region which include the two fields. It is read out at about 500 Hz. On the basis of these measurements, the correction in tip/tilt is performed by the M6 mirrors (cf. §3.4).

3.6 Fringe tracker

The fringe tracker module is composed of the beam combiner, two spectrometers, dichroic plates, multimode fibers and analog single pixel PIN detectors. The fringe sensor uses the four $\pi/2$ phase-shifted outputs (ABCD outputs) of the beam combiner, which perform a spatial modulation (already investigated for stellar interferometry on the ground [15]). After reflection on D2, the beams are sent pairwise through the spectrometers where dichroic plates separate them in two spectral channels (I and J). Then, light goes through small lenses and is injected into multimode fibers. Those fibers lead the light to Silicon (I band) and InGaAs (J band) analog single-pixel PIN detectors [12]. On the basis of these measurements, the correction in opd (piston) is done (cf. §3.4).

3.7 IR detection

The IR detection uses the nulled (D) and bright (B) outputs of the beam combiner in the H, K and L bands. SMFs are used to lead the light towards the detector. Then, they are linked together and reimaged on the camera. The fringes of D output are dispersed thanks to a direct-vision prism. It allows simultaneous access to all IR channels.

For the H and K bands, the detector is a camera using a Picnic 256x256 focal plane. This camera has a very low noise, which allows excellent signal to noise ratio (SNR) with a high frequency passband in the nulling mode (SNR > 20 at 100 Hz). It will improve the results in comparison with the previous systems based on single-pixel detectors (SYNAPSE [10], MAII [9]). It also allows the interferometer to have a lower transmission: about 1% from M1 to the detection and 0.05% from the source to the detection, including the quantum efficiency of the detector.

An InSb single-pixel detector from Judson is considered for the L band. Performances will be reduced to SNR \approx 10 at 0.5 Hz.

3.8 Computer and electronics set-up

A PXI chassis from National Instrumente hosts the real-time LabVIEW software of the co-phasing system and electronics interface cards. It is linked to a standard PC. This computer hosts the Graphic User Interface in LabVIEW and allows flexible communications with

other modules, such as the IR camera or later the GNC simulator. At first, we use datafiles of preliminary computed perturbations. All the electronics units, power supply and detectors (except the ST camera) are deported from the main optical bench not to disturb its stability.

3.9 Status of the modules

In the table 2, the status and the name of the consortium's members responsible of the development are listed for each module. The legend for the status is: D = under end of Definition, M = under Manufacturing, A = under Assembly.

Table 2: Status of PERSEE's modules

Module	Responsible	Status
Source and Separation	OCA	D
Optical train	OCA + TAS	D
ST system	ONERA	A
Combination	IAS+CNES+ONERA	D*
FT system	ONERA	A
IR detection	LESIA	M
Perturbation	TAS+LESIA+ONERA	D
Laboratory	LESIA	M

*optical components are under manufacturing

In the following parts, we describe in details the beam combiner and the fringe tracker.

4. THE BEAM COMBINER

The beam combiner has two functions:

- to provide a nulled achromatic output (D) and a constructive achromatic output (C) in the IR scientific range to perform nulling interferometry
- to generate four ABCD outputs [16] spatially in the FT range.

The challenge of the concept is to couple these two functions in the same optical device in order to minimize the differential paths. It allows to reduce differential stability requirements between the co-phasing metrology and the nulling interferometer. The nuller and the fringe sensor share the same optical components [18].

4.1 Optical design

The chosen design for the beam combiner is based on the Modified Mach Zehnder interferometer (MMZ) concept proposed by Serabyn and Colavita in 2001 [11]. This type of interferometer was tested during the study of the laboratory performance of the Keck Nuller [17] and on the "nulling bench" SYNAPSE (10^{-4} nulling level in the K band) [10]. It allows an optimally symmetric beam combination in terms of phase, amplitude and polarization, which are required for deep nulling interferometry. This geometry has been improved to reach the specifications of PERSEE [18]. The Fig. 3 shows the design of the optical device.

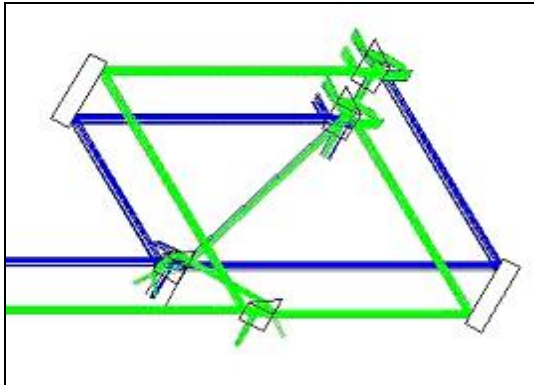


Fig. 3: Optical design of the PERSEE's beam combiner

This design is compact and the property of symmetry is maintained. The beam combiner is composed of 4 beam splitters and 2 mirrors. The 45° incidence angle of the classical Serabyn-Colavita's configuration hasn't been maintained [11], although it allows for a simple, more compact and easier to align geometry. We opted for 30° which is a trade-off to have a good balance between s and p polarization transmission and reflection factors.

4.1.1 The $\pi/2$ phase-shift

To produce the $\pi/2$ phase-shift between the four ABCD outputs of the FT, we introduce an opd of $\lambda/4 \pm 50$ nm at $\lambda = 1$ nm between the BD and AC outputs. The stability of the AC optical path has to be better than 0.5 nm rms with respect to BD. An appropriate and very precise positioning of one of the beam splitters allows to generate this opd.

4.1.2 Beam splitters geometry

The four beam splitters have a trapezoidal geometry [18] (cf. Fig. 4) to avoid stray light. The principle is to combine this design with an adequate thickness (> 10 mm) in order to eliminate the major part of stray light collinear to the main beams.

This concept has been implemented and successfully tested on the SYNAPSE test bench [10].

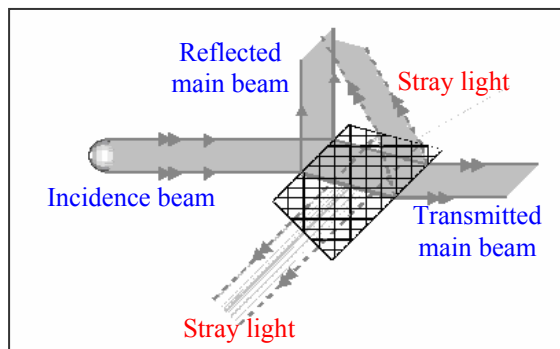


Fig. 4: Trapezoidal geometry of the beam splitters

4.2 Substrates and coatings

The substrate of the beam splitters is CaF_2 ($n \approx 1.4$ at $\lambda = 2 \mu\text{m}$). It has been chosen because of its low index of refraction. Concerning the coatings, the difficulty is to find some that would cover the whole spectral range of the nuller and the FT ($[0.8 - 3.3] \mu\text{m}$) with adequate phase dispersion properties. In order to reach desired performances, the rt product has to be greater than 0.17 between $1.65 \mu\text{m}$ and $3.3 \mu\text{m}$ and greater than 0.12 between 0.8 to $1.5 \mu\text{m}$. After several studies, we have opted for a three-layer Si-SiO₂ coating with a few 10^{-10} m rms uniformity of the layer thickness.

Concerning the mirrors, the selected substrate is Zerodur because of its extremely low thermal expansion coefficient. The coating is unprotected gold with a reflection coefficient better than 0.97 in the whole spectral range.

4.3 Mechanical Design

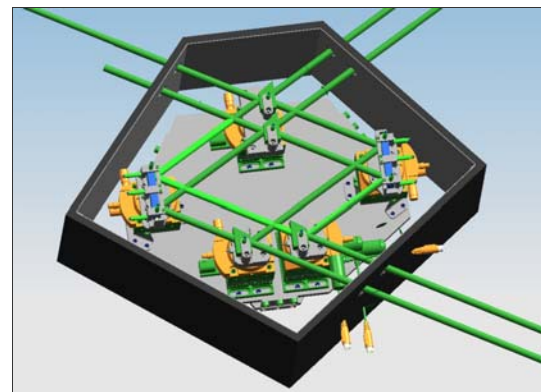


Fig. 5: Mechanical design of the beam combiner

The requirements in term of maximum positioning tolerances and stability that the beam combiner could accept in order to achieve the predicted performances have been determined [18]. Thanks to an appropriate design, we could minimize the differential opd between IR and SF channels and make the system intrinsically very stable. All the plates are on a special breadboard for a better stability. The whole device is enclosed in a protective housing to improve the thermal stability (cf. Fig. 5). This design has currently reached its final stages at IAS.

4.4 Status

The beam combiner is jointly developed by IAS, CNES and ONERA. IAS is also in charge of the supervision of manufacturing. It should be ready for integration on PERSEE and for its first tests in January 2009. In parallel, ONERA has developed a prototype to validate the FT system [12]. Its first results are described in §6.

5. THE FRINGE TRACKER

The fringe tracker is one of the key components of PERSEE. It belongs to the co-phasing system [12]. Its

goal is to minimize the mismatch path with respect to the science channel. The co-phasing system is implemented within two parallel servo loops: the OPD control loop (FT) and the tip/tilt control loop (ST). Preliminary results of this last loop are presented in [8]. The fine loops compensate the external disturbances by corresponding displacements of optical delay lines and fast steering mirrors. The optical components which perform these corrections are detailed in §3.4.

5.1 Specifications

The fringe sensor operates in $[0.8 - 1.5] \mu\text{m}$. In order to reach an average null depth of 10^{-4} with a 10^{-5} stability, the residual OPD must be lower than 2 nm rms. To reach this specification, two correction levels are implemented: a centimetric level with an accuracy of $\sim 1 \mu\text{m}$ and a nanometric level with an accuracy of 0.2 nm. The system operates within three modes described below.

5.1.1 Detection mode

Detecting the fringes is the first step to perform in interferometry. In this mode, the loop is open. When the star (on each arm) or fringes are detected (for example when the SNR of fringe visibility is larger than 5), their drift speed and direction are estimated and the acquisition mode is activated. For the ST, the field of the camera and the accuracy of the absolute positioning system should make this task easy. Things are more difficult for the FT as the ratio between the coherence length and the opd uncertainty is much lower. It is thus necessary to perform a fringe search, by moving the ODL with a linear scan or waiting for the fringes to pass while the spacecrafts drift.

5.1.2 Acquisition mode

At the begin beginning of the acquisition phase, the opd between the two arms of the interferometer can be much larger than the FT operating wavelength. The goal of this phase is to locate the central dark fringe and to decrease the opd under the FT operating wavelength. To do so, the FT spectral band is dispersed into two spectral channels. When the opd residual is lower than a fraction of the FT operating wavelength, the system automatically goes through the tracking mode.

5.1.3 Tracking mode

The tracking phase is the period during which the fringes are stabilized and the science channel makes observations. The main requirements are that the residual opd must be lower than 2 nm rms and the star position stabilized at 600 mas. To reach these specifications, it has been specified that the phase tracking must be performed with a sampling rate close to 1 kHz. Finally, in the case of fringe jumps, the dispersion will ensure dark fringe tracking by removing the main ambiguities.

5.2 Design of the Fringe sensor

As we have already said (cf. §4), the fringe tracker shares optical components with the scientific channel. The beam combination is performed by a kind of modified-Mach-Zehnder interferometer. The demodulation is carried out by the ABCD algorithm [12], the $\{0 - \pi/2 - \pi - 3\pi/2\}$ modulation is performed by adding a $\pi/2$ phase-shift in the beam combiner. Real time computing is carried out by the software LabVIEW Real Time running on a PXI chassis.

6. FIRST RESULTS OF THE CO-PHASING SYSTEM

A preliminary integration of the co-phasing system is currently performed at ONERA, based on the setup shown in Fig. 6. The (blue) light from a laser diode is injected through an output of the MMZ and the two generated beams are used as input (red) beams after autocollimation on the S316 mirrors. The star sensor is fed by a beam splitter, which also generates the pointing reference by retro-reflection of the illumination beams (dashed lines). The green beams are used to align the MMZ on a large reference mirror with an autocollimator. Since tests are done in parallel of the MMZ manufacturing, a dedicated MMZ has been developed by GEPI. It has been specially designed in order to reach the thermal stability requirement. GEPI has also manufactured the spectrometer blocs shown in grey-hatched in Fig. 6b.

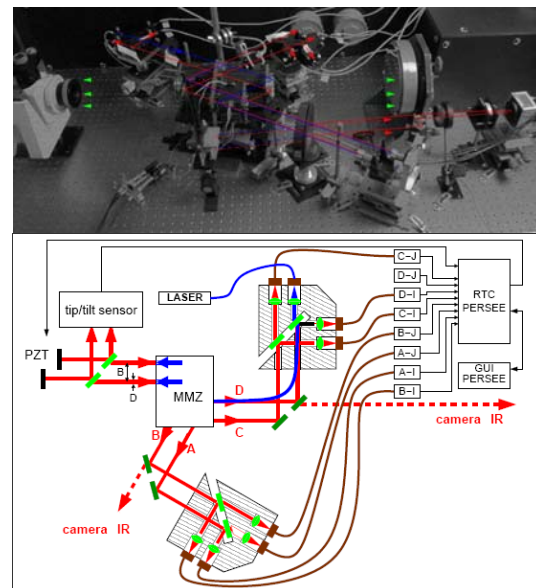


Fig. 6a and b: Photograph and diagram of the preliminary FT+ST integration at ONERA.

Using only two complementary outputs, the loop has very recently been closed with AC algorithm [19].

Fig. 7 shows a 50 second acquisition when the fringe tracker is successively:

- in open-loop: the measured phase induced by environmental perturbations is 12 nm rms
- in closed-loop, the environmental perturbations are reduced to 4.7 nm rms
- in open loop with a calibrated sinusoidal piston perturbation with an amplitude of 240 nm P-V.

It validates the successful operation of the fringe tracker with a bandwidth of only 5 Hz. A nanometric opd residue with a 100 Hz bandwidth is expected when the FS will operate at its nominal sampling rate of 1 kHz after software optimization.

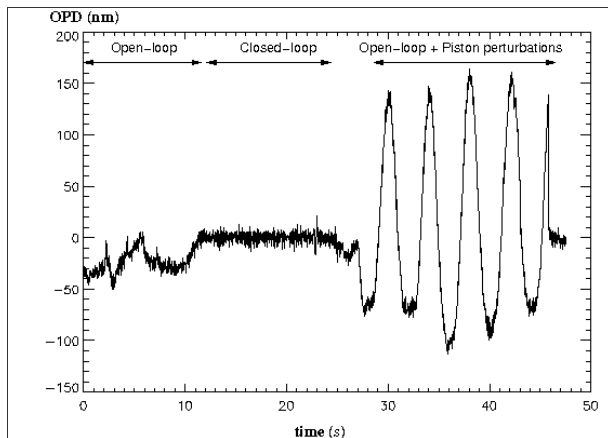


Fig. 7: First OPD tracking obtained at Onera

7. PERSPECTIVE

Bench development has currently reached its final stages and the integration of PERSEE will begin early 2009. Its first results are expected in mid 2009.

Concerning the beam combiner:

- the mechanical design should be ready mid-October
- the optical components are being manufactured
- the system should be ready for integration and first tests in January 2009.

ACKNOWLEDGEMENTS

Sophie Jacquinod's PhD Thesis is funded by CNES and TAS.

REFERENCES

1. Léger, A., et al., "Darwin: Mission concept for the ESA Horizon 2000+ program", ESA, 1993.
2. Léger, A., et al., "Darwin, a proposal for Cosmic Vision 2015-2025 ESA Plan", ESA, 2007.
3. Lawson, P. R. and Dooley, J. A., "Technology plan for the Terrestrial Planet Finder Interferometer", JPL 05-5, NASA, 2005.
4. Angel, J. P. R. and Woolf, N. J., "An Imaging Nulling Interferometer to Study Extrasolar Planets", *ApJ.*, 475..373A,1997.
5. Ollivier, M., et al., "PEGASE: an infrared interferometer to study stellar environments and low mass companions around nearby stars", proposal for Cosmic Vision 2015-2025 ESA Plan, ESA, 2007.
6. Le Duigou, J. M., et al., "PEGASE: a space-based nulling interferometer", *Proc. SPIE* 6265, pp. 62651M, 2006.
7. Danchi, W. C. and Lopez, B., "The Fourier Kelvin Stellar Interferometer (FKSI) – A practical infrared space interferometer on the path to the discovery and characterization of Earth-like planets around nearby stars", *Comptes Rendus Physique* 8, 396–407, Apr. 2007.
8. Cassaing, F. et al., "PERSEE: a nulling demonstrator with real-time correction of external disturbances", *Proc. SPIE* Vol. 7013, 70131Z, Jul. 28, 2008.
9. Weber, V., Barillot, M., et al., "Nulling interferometer based on an integrated optics combiner", *Proc. SPIE* 5491, pp. 842-850, 2004.
10. Brachet F., Etude et développement d'un déphaseur achromatique pour l'interférométrie en frange noire, PhD thesis, University of Paris-Sud (XI), 2007.
11. Serabyn, E. and Colavita, M. M., "Fully Symmetric Nulling Beam Combiners", *Applied Optics* 40, 1668-1671, Apr. 2001.
12. Houairi, K., "PERSEE, the dynamic nulling demonstrator: recent progress on the cophasing system", *Proc. SPIE* Vol. 7013, 70131W, Jul. 28, 2008.
13. Van den Dool, T. et al., "The darwin breadboard cryogenic optical delay line Darwin", ICSO 2006.
14. Villien, A. et al., "Gnc for the pegase mission," in [17th IFAC Symposium on Automatic Control in Aerospace], June 2007.
15. Cassaing, F., et al., "An optimized fringe tracker for the VLTI/PRIMA instrument," in [Interferometry in optical astronomy], Léna, P. J. and Quirrenbach, A., eds., 4006, 152–163, *Proc. Soc. Photo-Opt. Instrum. Eng.*, SPIE 2000.
16. Shao, M., Colavita, M. M., et al., "The Mark III Stellar Interferometer", *Astronomy and Astrophysics* 193, 357-371, 1988.
17. Mennesson, B., et al., "Laboratory performance of the Keck Interferometer nulling beam combiner", in *Towards Other Earths: DARWIN/TPF and the Search for Extrasolar Terrestrial Planets*, ed. M. Fridlund & T. Henning (ESA SP-539; Noordwijk: ESA), 525-528.
18. Jacquinod, S. et al., "PERSEE: description of a new concept for nulling interferometry recombination and OPD measurement", *Proc. SPIE* Vol. 7013, 70131T, Jul. 28, 2008.
19. Cassaing, F., "Optical path difference sensors," in [Comptes Rendus de l'Académie des Sciences], IV Physics, 1–12, 2001.